

Engineering Geology and Slope Stability of West Pit Coal Mine of PT. Tawabu Mineral Resource, East Kalimantan, Indonesia

Rama Tri Saksono, I Gde Budi Indrawan*, and Wahyu Wilopo

Department of Geological Engineering, Faculty of Engineering, Universitas Gadjah Mada, Yogyakarta, Indonesia

Received: July 24, 2022 / Accepted: January 2, 2023 / Published online: January 20, 2023

ABSTRACT. The research area was located in the west pit of the open pit coal mine of PT. Tawabu Mineral Resource (TMR) in Bengalon District, East Kutai Regency, East Kalimantan Province, Indonesia. Several landslides drove the research in the area; however, the remaining slopes' engineering geological conditions and stability have not been evaluated. This study's objectives were to understand better the engineering geological conditions and stability of the research area. The geological engineering conditions (i.e., geomorphology, rock and soil, geological structure, and groundwater conditions) were evaluated by photogrammetric analyses, field observations, and analyses of borehole logs and laboratory test results. The slope stability analyses were first carried out by conducting back stability analyses of failed slopes on the northern lowwall slope segment. The shear strength parameters obtained from the back analyses were then used for forward stability analyses of the remaining 10 lowwall and highwall slopes. The slope stability analyses involved deterministic and probabilistic analyses, under static and dynamic, using the limit equilibrium method (LEM). The results showed that the research area and the surroundings consisted of two geomorphological units: the alluvial plain and structural hills. Rocks in the study area consisted of claystone, sandstone, and coal with a general layer strike direction of N59°E – N63°E with a dip of 19°–26°. These rocks were grouped into two lithological units: alternating sandstone and claystone unit, and alternating claystone and coal unit. The geological structures were identified on the highwall, from west to east, namely a major sinistral shear fault with a relative direction of NNE–SSW, two minor sinistral shear faults with a relative direction of NE–SW, and a major dextral shear fault with a relative direction of NW–SE. These geological structures were interpreted as being formed by the folding process. The groundwater level was estimated at -45 m to 20 m. The slope stability analyses showed that only the East HW-4 slope, located on the east highwall, was unstable. It is recommended to optimize the slope by either lowering the groundwater elevation by 4 m from the actual level or by reducing the overall slope angle to 31°.

Keywords: Back stability analysis · Coal mine · Engineering geology · Forward stability analysis · Slope optimization.

1 INTRODUCTION

Characterization of geological engineering conditions needed to be carried out in evaluating

*Corresponding author: I G.B. INDRAWAN, Department of Geological Engineering, Universitas Gadjah Mada. Jl. Grafika 2 Yogyakarta, Indonesia. E-mail: igbindrawan@ugm.ac.id

slope stability at a research location. Ulusay (2013, 2019) emphasizes the importance of harmonizing engineering geology with rock engineering on the stability of natural and engineered rock slopes. Gonzalez de Vallejo and Ferrer (2011) explained that engineering geological investigations need to be carried out to

provide a geological and geotechnical description of the excavation area, to obtain the parameters needed for stability analysis, slope design, and stabilization and drainage measures. Some aspects of engineering geology that need to be investigated in slope stability analysis are geomorphological conditions, rock and soil conditions (stratigraphy, lithology, and geomechanical properties), geological structures, hydrogeological conditions, and other factors such as static and dynamic loads (Bell, 2007; Gonzalez de Vallejo and Ferrer, 2011).

Stacey (2010) stated that designing the slope of an open pit mine is aimed at providing optimal excavation configuration in the context of safety, ore/coal recovery, and financial return. Bell (2007) further emphasized that the stability of slopes is a critical factor in open excavation. The character of the rocks and soils and their geological setting must be investigated to accomplish optimum excavation economically and safely. Thus, evaluating the slope stability of the research location is crucial in ensuring that the safety and economic aspects of the mine are optimum.

The research location is in the West Pit of an open pit coal mine within the area of the Mining Business Permit (IUP) owned by PT. Tawabu Mineral Resources (TMR). Administratively, the research area is located in East Sepaso Village, Bengalon District, East Kutai Regency, East Kalimantan Province. Along with the progress of the mining process over the last few years at the research site, there have been several slope failures accompanied by the formation of tension cracks in the research area. This phenomenon signifies the importance of slope stability evaluation in the study area.

Several studies have been carried out around the research area, including geological mapping and coal resource calculations (Sandria, 2014), slope stability evaluation, and landslide volume prediction in the east pit (Santoso, 2022). However, no study has evaluated slope stability in the west pit of the PT. TMR. This research needed to be carried out as an evaluation of the condition of mine slope stability in accordance with the criteria specified in the Minister of Energy and Mineral Resources Decree of the Republic Indonesia No. 1827 K/30/MEM/2018 (ESDM Ministry, 2018), as well as providing

recommendations for optimization that can be done based on the results of the evaluation.

2 THEORY

Gonzalez de Vallejo and Ferrer (2011) describe that slope stability is influenced by geometric factors (height and angle), geological factors (which control the presence of surface and weak zones and anisotropy on slopes), hydrogeological factors (related to the presence of water) and geomechanical factors (strength, deformability, and permeability). Aspects of engineering geology can represent these factors. Geometric factors can be explained through geomorphological analysis, geological factors can be described through stratigraphic and structure analysis, hydrogeological factors are represented by groundwater table elevation analysis, and geomechanical factors are represented by index and mechanical properties. Gonzalez de Vallejo and Ferrer (2011) also explain that factors influencing slope stability can be characterized into 2 categories: conditioning factors and triggering factors. Conditioning factors are geological, hydrogeological, and geotechnical factors intrinsic to natural materials, while triggering factors are external factors that act on soils and rock masses, modifying their characteristics and properties and conditions of the slope equilibrium.

The limit equilibrium method (LEM) is commonly used for slope stability analyses. This method is relatively simple and reliable in modeling and predicting slope stability conditions. This allows the evaluation of several parameters that affect slope stability, such as natural stresses, dynamic forces, and water pressure (Gonzalez de Vallejo and Ferrer, 2011). Gonzalez de Vallejo and Ferrer (2011) also explained that the LEM analyzes potentially unstable masses by comparing the resisting forces with the tending to slide along a slip plane. The equilibrium equation between the resisting force and the driving force can be expressed as a factor of safety (FS), where $FS = 1$, indicating that the forces acting on the slope are in equilibrium. One widely used calculation technique in the LEM is the Morgenstern-Price equation (Morgenstern and Price, 1965). This formula considers the force equilibrium in the x and y

directions and the moment equilibrium (Lorig *et al.*, 2010; Abramson *et al.*, 2002).

This study also carried out probabilistic method calculation to accommodate the slope stability criteria specified in the ESDM Ministry (2018). The probabilistic method calculates the probability of a slope sliding under certain conditions, where the distribution function of the parameters taken into account must be known, which is considered a random variable in the analysis. The safety factor is calculated based on this function using an iterative process (Gonzalez de Vallejo and Ferrer, 2011). Probabilistic methods are generally used and aimed at statistically characterizing the safety factor for a statistical input of rock mass parameters (Abdulai and Sharifzadeh, 2019). There is a linear relationship between the probability of landslides and the occurrence of landslides, while on the other hand, there is no definite relationship between the safety factor and the occurrence of landslides (Tapia *et al.*, 2007; Abdulai and Sharifzadeh, 2019). In the probabilistic method, the level of slope stability is defined in terms of Probability of Failure (PoF or PF), which shows the ratio between the number of model simulations experiencing failure ($FS < 1$) and the total number of simulations. The deterministic concept has been described by Tapia *et al.* (2007) and Steffen *et al.* (2008). The slope stability criteria used in this study refer to the Guidelines for implementing Good Mine Engineering Rules specified in the ESDM Ministry (2018).

The slope stability criteria are determined based on the type of slope and the consequence of failure (CoF), with criteria in the form of minimum static FS, minimum dynamic FS, and maximum PF. In this study, slope stability analysis was carried out on the overall slope with a low CoF. Thus, the criteria used are as follows:

- Minimal $FS_{static} = 1.2-1.3$
- Minimal $FS_{dynamic} = 1.0$
- Maximum PoF = 15–20%

3 LOCATION AND REGIONAL GEOLOGY OF STUDY AREA

The research location is the West Pit of an open pit coal mine covering an area of 0.31 km²

which is in the area of the Mining Business Permit (Izin Usaha Pertambangan/IUP) owned by PT. Tawabu Mineral Resources (TMR). This location is administratively located in East Sepaso Village, Bengalon District, East Kutai Regency, East Kalimantan Province. The research site is located about 1.8 km to the east of the confluence of the Keraitan River with the Bengalon River or about 20 km to the north of the city of Sangatta, the capital of East Kutai Regency. The map of the research location is shown in [Figure 1](#).

Based on the physiography, the research area is located in the Lower Kutai Basin (Nuay *et al.*, 1985 in Bachtiar, 2004; Moss and Chambers, 1999). According to Moss and Chambers (1999), the Lower Kutai Basin is bounded by 2 fault zones with an NW–SE trend, the Sangkulirang Fault in the north and the Adang Fault/Adang Flexure in the south. These fault zones and their offsets extend toward land and sea (Cloke *et al.*, 1999). There is a Bungalun/Bengalon lineament with a relatively NW-SE direction which controls the direction of the Bengalon River flow.

Based on the Geological Map of Sangatta No. 1916 with a scale of 1:250000 (Sukardi *et al.*, 1995), the rocks in the study area consist of the Menumbar Formation (Tmme). This formation is composed of alternating chalky mudstones with limestone at the bottom and, at the top massive sandstones containing glauconite, which exhibits cross-bedding. Chalky mudstone indicates the age of the upper Middle Miocene to the lower Late Miocene. The upper part of this formation is found to be interfingered with the Balikpapan Formation (Tmbp). Menumbar formation was deposited in an inner to the outer neritic marine environment, with a rock thickness of about 1000 meters.

There is no major geological structure in the study area. However, according to Sukardi *et al.* (1995) and Bachtiar *et al.* (2013a, 2013b), there are several geological structures scattered around the study site, most of them are fold systems (anticline and syncline), and there is a Bengalon sinistral strike-slip fault to the southwest of the study area.

4 METHODS

The research went through two stages: data collection and analysis. The following is the se-

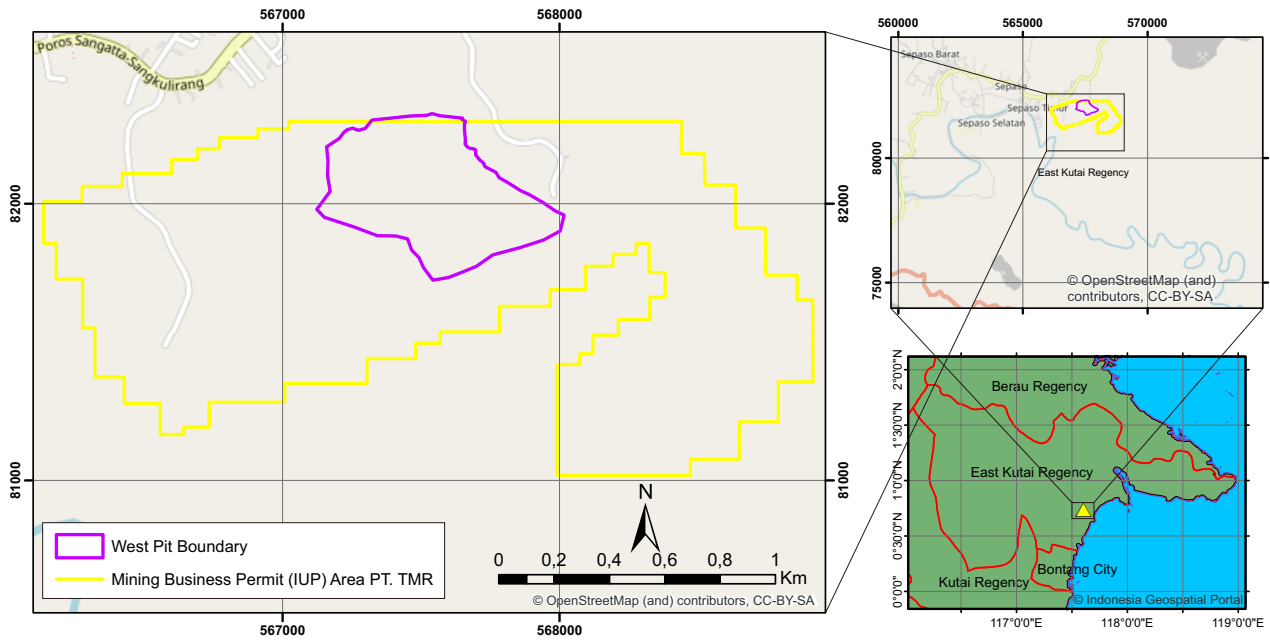


FIGURE 1. Location map of the research area.

quence of stages of research and the work carried out at each stage. In the data collection stage, secondary data and primary data used in the analysis phase were collected. Secondary data includes pre-mining and post-mining topographic maps, CPT data, drilling data, laboratory test results of physical and mechanical properties, earthquake loads as dynamic loads, heavy equipment loads as static loads, and previous geological investigations. Primary data includes aerial photographs using UAV/drone and observing geological field conditions. Aerial photographs were taken vertically in bright lighting conditions for resulting good photos. A total of 381 aerial photos were taken on 9 February 2022 and 146 aerial photographs on 11 February 2022, and these two data complement each other in their use in further analysis. Aerial photographs are processed in Agisoft Metashape Professional software version 1.8.0 to produce orthomosaic, 3-dimensional models and DEM. The data collected through aerial photography is carried out because this method is safer, considering the condition of the research location, which is an active operational mine with slope stability condition that has not been verified. In addition, this method allows observations to be more efficient in terms of time and can observe areas that are difficult to access in the field.

In the analysis stage, an analysis of geological

engineering conditions is carried out, including geomorphological analysis (i.e., drainage patterns, lineament patterns, slopes), rock and soil analysis (stratigraphy, index, and mechanical properties), geological structure analysis (i.e., type, location, and orientation of faults), and analysis of groundwater table elevation. The geomorphological analysis was done by analyzing the pre-mining topography and DEM. The rock and soil analysis was done by analyzing geological observation from field observation and aerial photographs, CPT, drilling, and laboratory results. The determination of rock units followed the guidelines given by the Indonesian Stratigraphy Code (IAGI, 1996) regarding unofficial rock units. Rocks in the study area were divided based on lithostratigraphic units, which are intended to classify rocks systematically into named units based on lithological characteristics. The structural geology analysis was done by analyzing geological observations from field observations and aerial photographs. The groundwater level analysis was done by plotting and interpolating the elevation of 40 sample points of surface water ponds which were assumed to be a manifestation of groundwater evidenced by seepages around the ponds, as there were no available groundwater level measurements. These analyses explain engineering geological conditions and considerations in modeling slope

stability. Slope stability analysis was carried out using the deterministic LEM method and the probabilistic method using the Rocscience Slide software. The deterministic analysis was carried out using the Morgenstern-Price equation. Probabilistic analysis was carried out using the sampling method with a Monte-Carlo simulation of 1000 samples. Slope stability analysis was carried out on 10 profiles representing the Lowwall (LW), East Highwall (East HW), and West Highwall (West HW) segments to obtain the Factor of Safety (FS) and Probability of Failure (PoF) values. These values were then compared with the criteria for slope stability of the ESDM Ministerial Decree No. 1827 K/30/MEM/2018 (ESDM Ministry, 2018) to identify unstable slope segments for further recommendations for slope design optimization.

5 RESULTS AND DISCUSSION

5.1 Engineering geological conditions

The results of the photogrammetric analysis of the research area are shown in [Figure 2](#), which shows the mine situation, pit boundary, slope stability analysis profile lines, drilling points, CPT points, landslide delineation, fault offsets, and surface water pond boundaries. Based on the photogrammetric analysis, several circular landslide bodies were identified in the research area, located on the slopes of the southern Highwall, northern Lowwall, and western Lowwall. Some landslides are associated with tension cracks and surface water ponds. The relatively large landslides occur on the Lowwall slope (northern slope), which tends to be gentler than the Highwall slope (southern slope). Landslides in this zone are interpreted to occur due to weak areas along the saturated rock layers with associating tension cracks. The presence of a water-saturated zone is characterized by the presence of standing water at the top and foot of the slope. A detailed aerial photograph showing the landslide delineation is shown in [Figure 3](#).

Geomorphological analysis was carried out to estimate the subsurface geological conditions manifested in the geomorphological conditions on the surface through the study of DEM data and pre-mining topography. The geomorpho-

logical analyses carried out in this study were the analysis of drainage patterns, morphological lineament patterns, slope class, and the determination of geomorphological units. The drainage pattern map of the research location is shown in [Figure 4](#). Based on this map, the upstream of smaller intermittent tributary rivers originates from hill inlets which generally face each other and meet on longer subsequent intermittent rivers, which are relatively parallel to the longitudinal direction of the hills. Surface meteoric water (runoff) that falls on the top of the hills then descends through the recesses of the hills. These recesses are interpreted to be formed due to the presence of joints and faults that are permeable zones and more easily eroded than the surrounding zone. Based on intermittent river delineation, the drainage pattern that developed at the research site was trellis. According to Howard (1967), the trellis pattern is caused by several geological controls, including dipping or folded sedimentary rocks and areas with parallel fractures. The modified drainage pattern relevant to the study area's geomorphological conditions is a directional trellis formed due to the influence of homocline morphology with a gentle slope. The morphological lineament pattern map that has been analyzed is shown in [Figure 5](#). Generally, the morphological lineament pattern in the surrounding research area has the main trend of NW-SE and NE-SW. The drainage pattern map of the research location is shown in [Figure 6](#). Based on this map, the upstream of smaller intermittent tributary rivers originates from hill inlets which generally face each other and meet on longer subsequent intermittent rivers, which are relatively parallel to the longitudinal direction of the hills. Surface meteoric water (runoff) that falls on the top of the hills then descends through the recesses of the hills. These recesses are interpreted to be formed due to the presence of joints and faults that are permeable zones and more easily eroded than the surrounding zone. The drainage pattern developed at the research site was trellis based on intermittent river delineation. According to Howard (1967), the trellis drainage pattern is caused by several geological controls, including dipping or folded sedimentary rocks and areas with parallel fractures. The modified

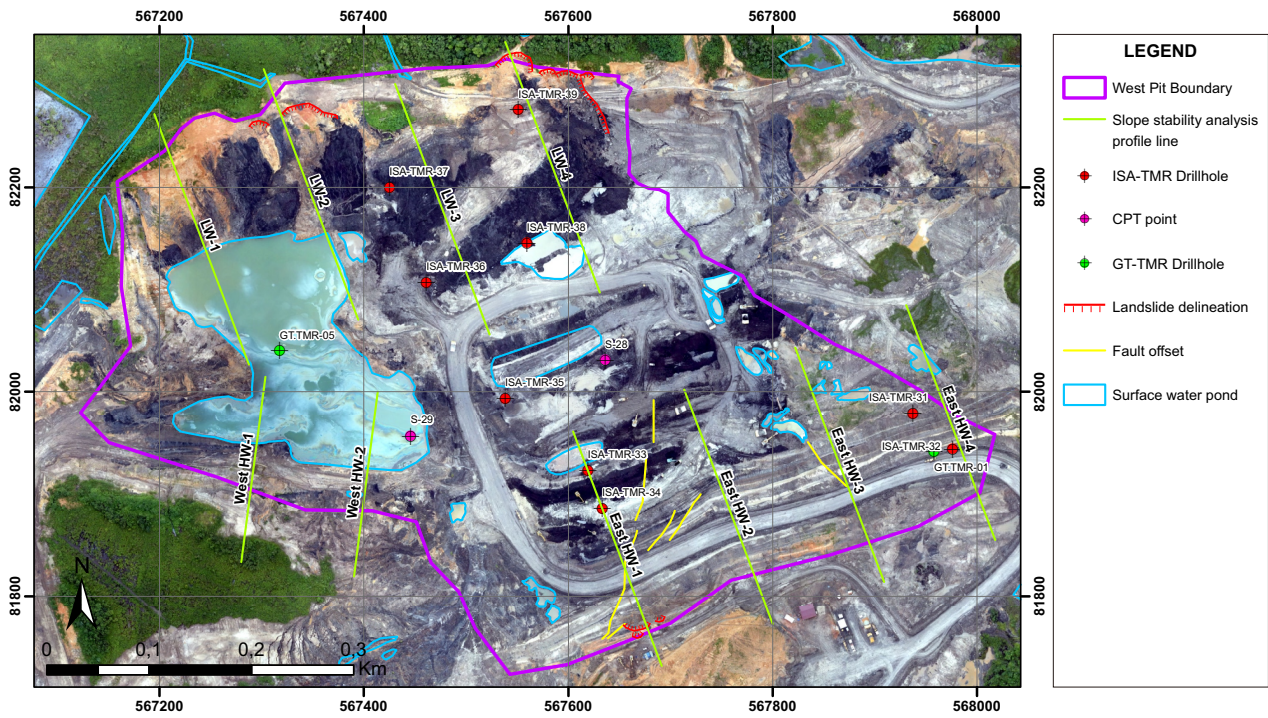


FIGURE 2. Photogrammetry analysis map of the research area.

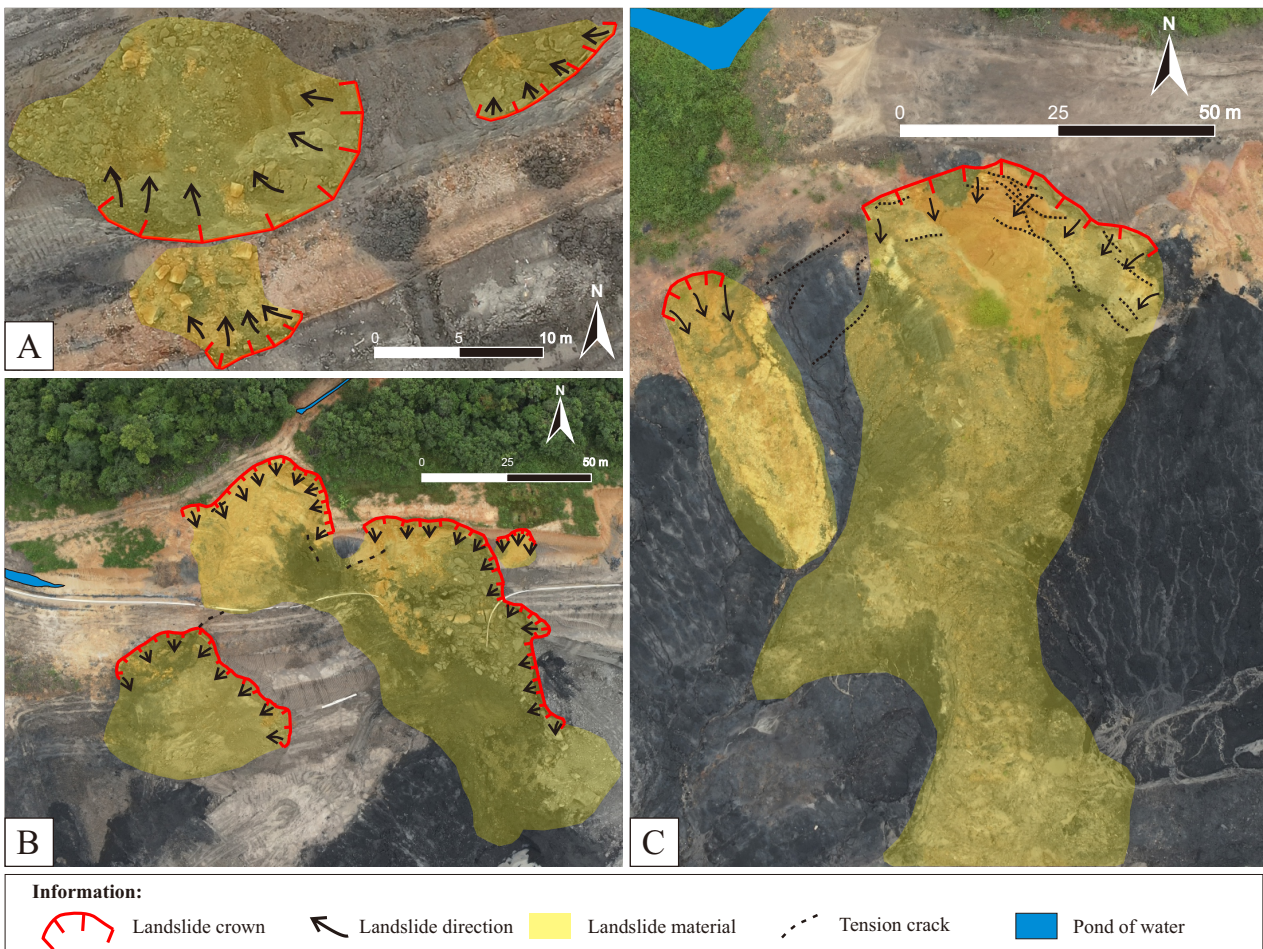


FIGURE 3. Aerial photographs showing landslide delineation in (A) southern Highwall; (B) northern lowwall; (C) western Lowwall.

drainage pattern relevant to the study area's geomorphological conditions is a directional trellis formed due to the influence of homocline morphology with a gentle slope. Based on the standardized geomorphological classification for geological mapping (Bermana, 2006), the main aspects analyzed in geomorphological mapping are morphology/morphography, morphometry, and morphogenesis. Two geomorphological units have been identified at the study site: an alluvial plain and structural hills. Based on Van Zuidam slope classification (1983), the alluvial plain unit has a flat to gentle slope (0–7%), while the structural hills unit has a slightly steep to the steep slope (more than 14%). The distribution of pre-mining geomorphological units in the study area is shown on the geomorphological map (Figure 6).

Rock conditions include determining rock units and the index and mechanical properties of rocks at the research site. The stratigraphic layer of rocks in the research area generally has a strike ranging from N59°E – N63°E with a dip of 19°–26°. There were few variations in the direction of bedding observed at the research site, so the bedding tends to be uniform. The lithology found at the research site generally consists of claystone, sandstone, and coal. The following is a general description of each lithology encountered at the study site:

- Claystone: light gray – brownish gray; lamination and bedding structures; clay grain size (<1/256 mm), good sorting, closed fabric; composed of clay minerals and organic material.
- Sandstone: yellowish white – brownish white; cross-bedding structure; fine – medium grain size, good sorting, closed fabric; composed of the siliciclastic mineral.
- Coal: dark gray – black; bedding structure; clay grain size (<1/256 mm), good sorting, closed packaging; organic material composition.

Based on the collection of lithological types, there were 2 rock units identified, from old to young, namely the alternating claystone and coal unit, then the alternating sandstone and claystone unit. The unit boundary was marked

by the occurrence of a sandstone layer which becomes the keybed along the strike plane of the bedding. The distribution of these two rock units is shown on the geological map of the research area (Figure 7). The geological profiles A–A' and B–B' are shown in Figure 8. The index and mechanical properties used in the slope stability analysis were obtained based on the results of laboratory tests of drilling samples, summarized in Table 1. There are no statistical parameters for coal because there was only 1 available sample.

Field observations and aerial photo analysis identified several strike-slip faults along the Highwall slope south of the research area (Figure 7). The faults identified from west to east were: a major oblique sinistral shear fault with an NNE–SSW direction (called Fault 1), 2 minor sinistral shear faults with a NE–SW direction, and a major dextral shear fault with an NW–SE relative direction (called Fault 2). Faults 1 and 2 were assumed to be conjugate faults in contact with each other. Stereographic analysis of conjugate faults showed that the major, intermediate, and minor principal stresses (σ_1 , σ_2 , and σ_3) have N43°E, N168°E, and N264°E orientations, respectively (Saksono, 2022). The formation of geological structures at the research location can be interpreted and explained using Stearns' Model, as explained by Saksono (2022). This model was developed by Stearns (1968), summarized by Bergbauer and Pollard (2004), and redefined by Davis *et al.* (2012). The model explained the fracture patterns (joints and faults) that can develop in rock layers during forming of large anticline structures. The rock layers at the research location are assumed to be anticline limbs based on regional geological conditions around the study site, indicating the presence of folding systems (Sukardi *et al.*, 1995). Based on the Stearns Model, the research location is characterized as System 2, where there are 2 sets of conjugate faults (Fault 1 and Fault 2) and 1 set of mode I tensile joints (represented by the NE–SW lineament pattern and minor sinistral strike-slip NE–SW faults). This system is located above a 'neutral surface' in the stretching zone.

The groundwater level (GWL) analysis results are displayed on the map of groundwater elevation and flow interpretation of the re-

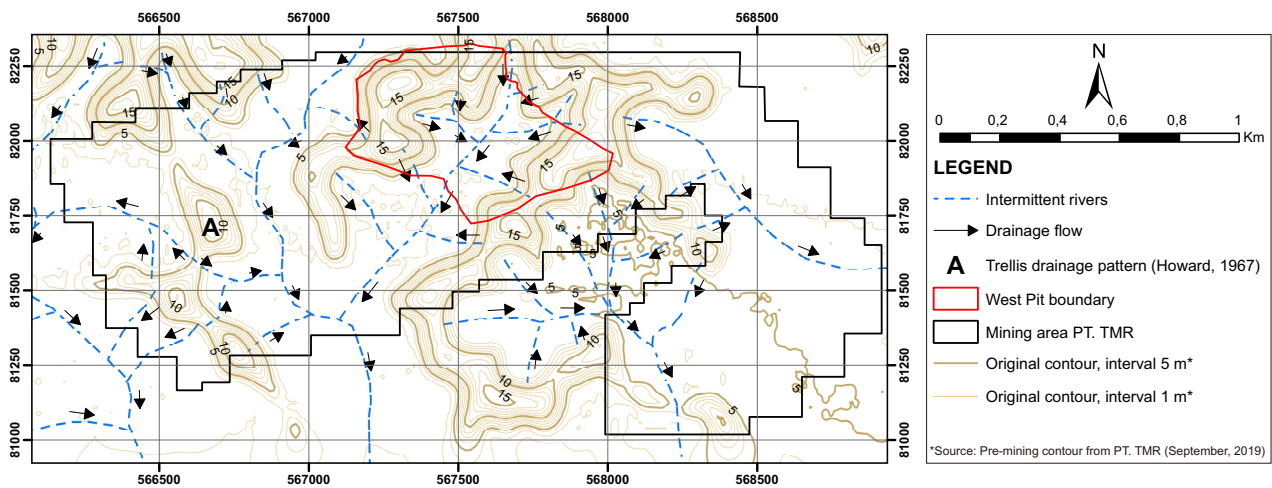


FIGURE 4. Drainage pattern map of the research area.

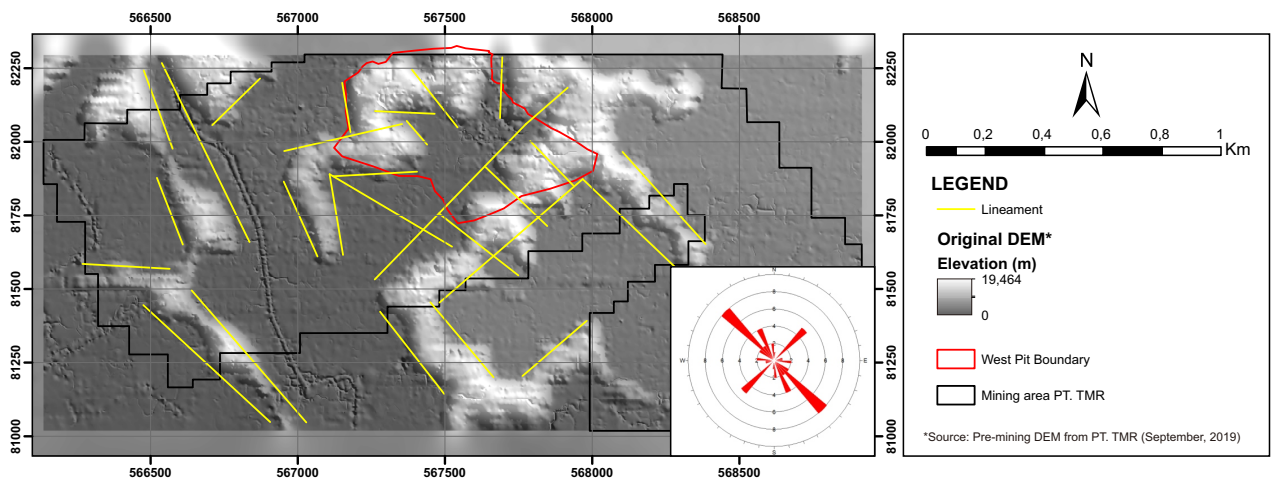


FIGURE 5. Morphological lineament pattern map of the research area.

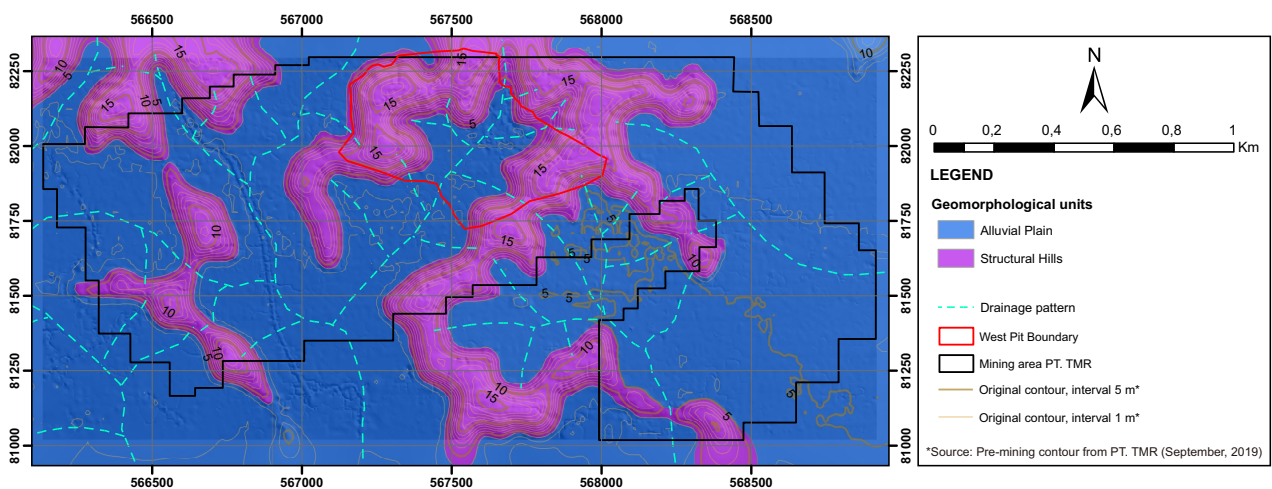


FIGURE 6. Geomorphological map of the research area.

ENGINEERING GEOLOGY AND SLOPE STABILITY OF WEST PIT COAL MINE OF PT. TMR

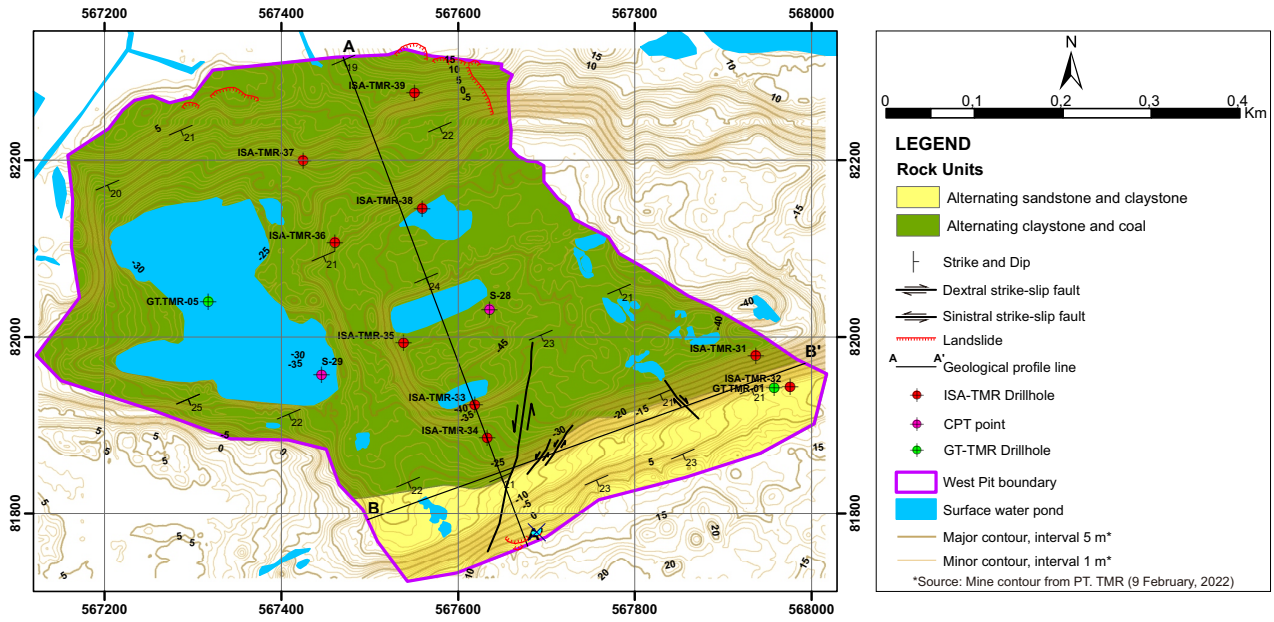


FIGURE 7. Geological map of the research area.

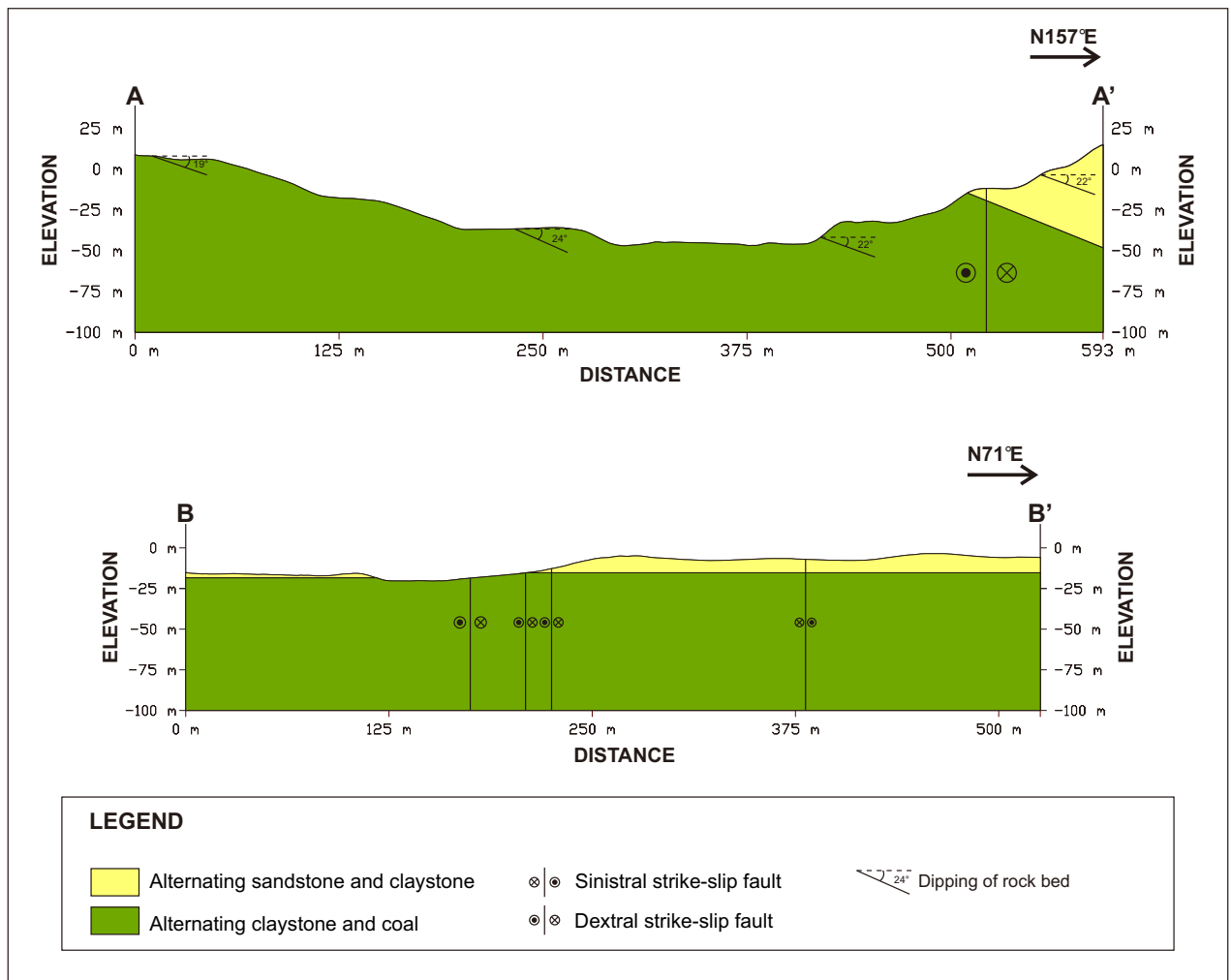


FIGURE 8. Geological profiles of A-A' and B-B'.

TABLE 1. Statistics of material design parameters based on laboratory test results.

| Material | Parameter | Min | Max | Mean | Standard Deviation | Coefficient of Variation (COV) | Characteristic value, x_k (Schneider, 1997) | |
|-----------|--|--------------|-------|--------|--------------------|--------------------------------|---|--------|
| Claystone | Unit weight, γ (kN/m ³) | 17.30 | 20.90 | 19.09 | 1.00 | 0.05 | 18.59 | |
| | Peak shear strength | c_p (kPa) | 45.40 | 297.14 | 131.71 | 74.42 | 0.57 | 94.50 |
| | | ϕ_p (°) | 18.00 | 40.78 | 30.47 | 7.15 | 0.23 | 26.89 |
| | Residual shear strength | c_r (kPa) | 33.54 | 172.30 | 88.92 | 41.68 | 0.47 | 68.08 |
| | | ϕ_r (°) | 12.50 | 29.25 | 21.36 | 5.29 | 0.25 | 18.71 |
| Sandstone | Unit weight, γ (kN/m ³) | 16.17 | 19.36 | 18.35 | 1.15 | 0.06 | 17.78 | |
| | Peak shear strength | c_p (kPa) | 88.26 | 326.56 | 166.79 | 113.42 | 0.68 | 110.09 |
| | | ϕ_p (°) | 27.92 | 40.44 | 35.28 | 5.87 | 0.17 | 32.35 |
| | Residual shear strength | c_r (kPa) | 43.25 | 183.87 | 114.36 | 58.00 | 0.51 | 85.37 |
| | | ϕ_r (°) | 21.64 | 31.34 | 26.18 | 3.63 | 0.14 | 24.37 |
| Coal | Unit weight, γ (kN/m ³) | - | - | 16.43 | - | - | - | |
| | Peak shear strength | c_p (kPa) | - | - | 61.49 | - | - | |
| | | ϕ_p (°) | - | - | 27.92 | - | - | |
| | Residual shear strength | c_r (kPa) | - | - | 42.27 | - | - | |
| | | ϕ_r (°) | - | - | 18.02 | - | - | |

search area (Figure 9). The GWL elevation in the study area was interpreted to range from -45 m to 20 m above sea level. Areas outside the pit boundaries generally had a groundwater level of more than 0 m. The lowest GWL elevation was at -45 m levels which were interpreted as being located in the middle of the research area, which was manifested as a water pond experiencing groundwater seepage from the surrounding rocks.

5.2 Slope Stability

Back analysis was carried out on the lowwall slope represented by the LW-4 profile (the location of the profile can be seen in Figure 2). Several landslides are identified around this slope segment, one of which is a landslide cut off by the LW-4 profile. Field observations and aerial photographs show that these landslides occurred in claystone, sandstone, and coal layers.

Back analysis was carried out by reducing the rock shear strength parameter until it was close to reaching the critical condition (FS = 1.0) to simulate the slope condition when the landslide occurred. Slope stability analysis of LW-4 using the peak shear strength parameter, which was characterized according to the method of Schneider (1997), as shown in Table 2, resulted

in the value of FS = 1.25. Back analysis was then carried out by reducing the rock shear strength parameters. The sensitivity curve of the claystone and sandstone shear strength parameters is shown in Figure 10. Coal shear strength parameters were not included in this curve because there was only 1 test data, and unable to be characterized statistically. Based on this curve, the cohesion parameter (c) of claystone is the most sensitive parameter, followed by the angle of friction (ϕ) of claystone. Parameters c and ϕ of sandstone appeared to show low sensitivity to changes in slope safety factor. Based on this information, parameter reduction was carried out on the claystone shear strength parameters. Several trials on reducing the shear strength parameter have been carried out until finally, it was found that a 20% reduction in the claystone peak shear strength parameter resulted in a safety value close to critical, where FS = 1.052. The design parameters of the back analysis results are shown in Table 2. The back analysis model for slope stability LW-4 is shown in Figure 11.

Slope stability analysis was carried out on 10 profiles representing highwall and lowwall slope segments. Slope material design parameters used the value of the back analysis results in Table 2. The highwall slope is located

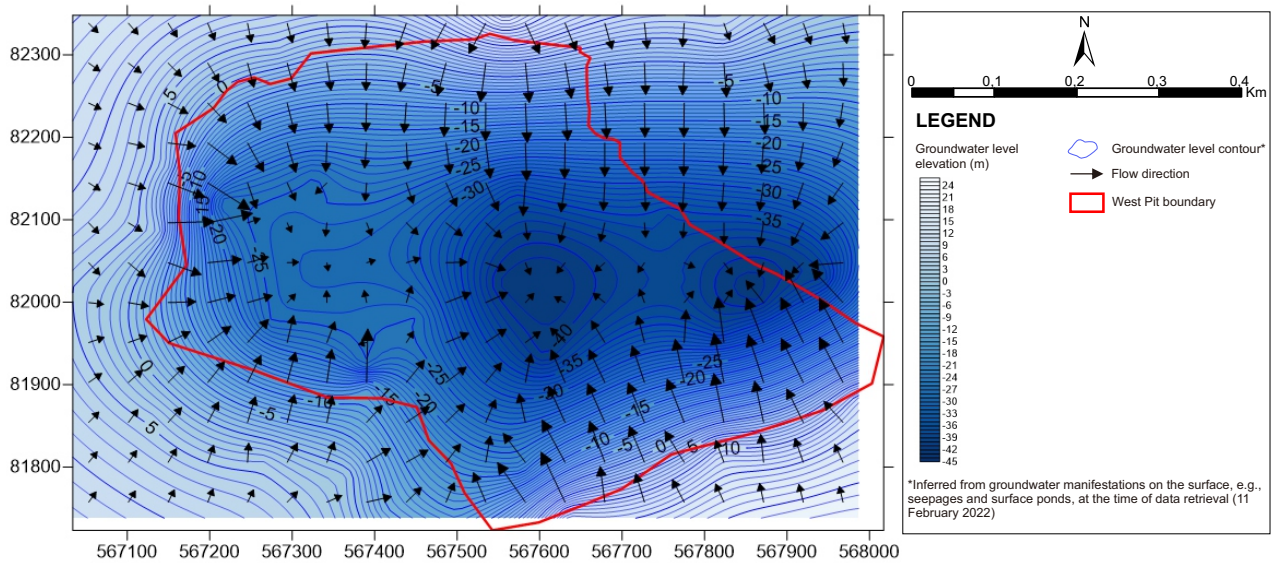


FIGURE 9. Map of groundwater level elevation and flow interpretation of research area.

TABLE 2. Parameters of rock shear strength resulting from back analysis of LW-4 profile.

| Material Name | Color | Unit Weight (kN/m ³) | Strength Type | Cohesion (kPa) | Phi (deg) | Water Surface | Hu Type |
|---------------|--------|----------------------------------|---------------|----------------|-----------|---------------|----------|
| Claystone | Green | 18.59 | Mohr-Coulomb | 75.6 | 21.512 | Water Surface | Constant |
| Sandstone | Yellow | 17.78 | Mohr-Coulomb | 110.09 | 32.34 | Water Surface | Constant |
| Coal | Black | 16.426 | Mohr-Coulomb | 61.487 | 27.92 | Water Surface | Constant |

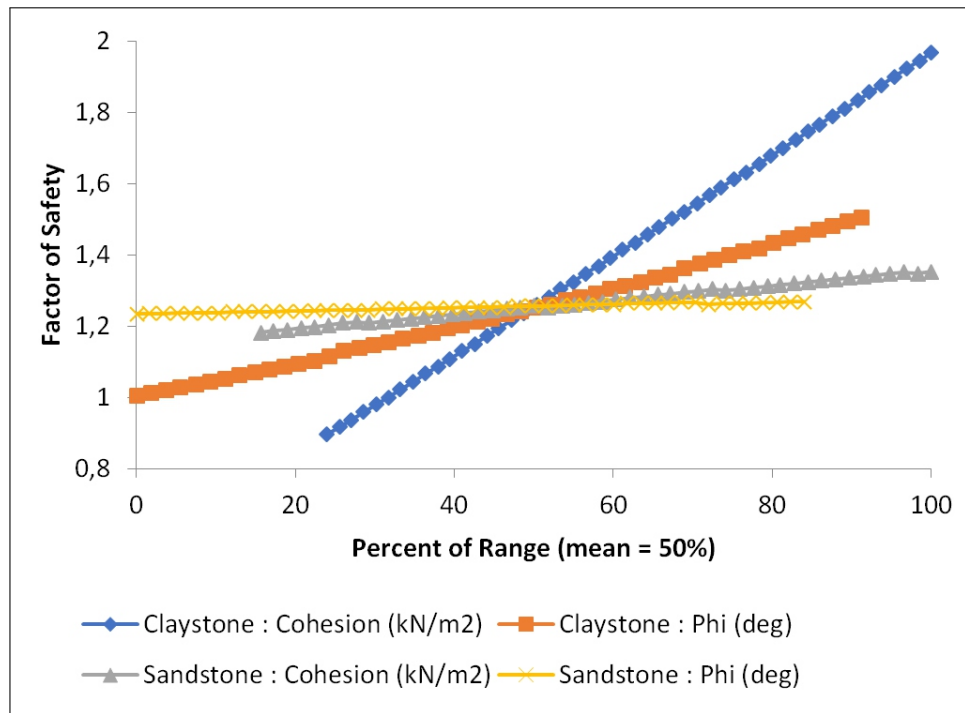


FIGURE 10. The sensitivity curve of the peak shear strength parameter to the slope safety factor LW-4.

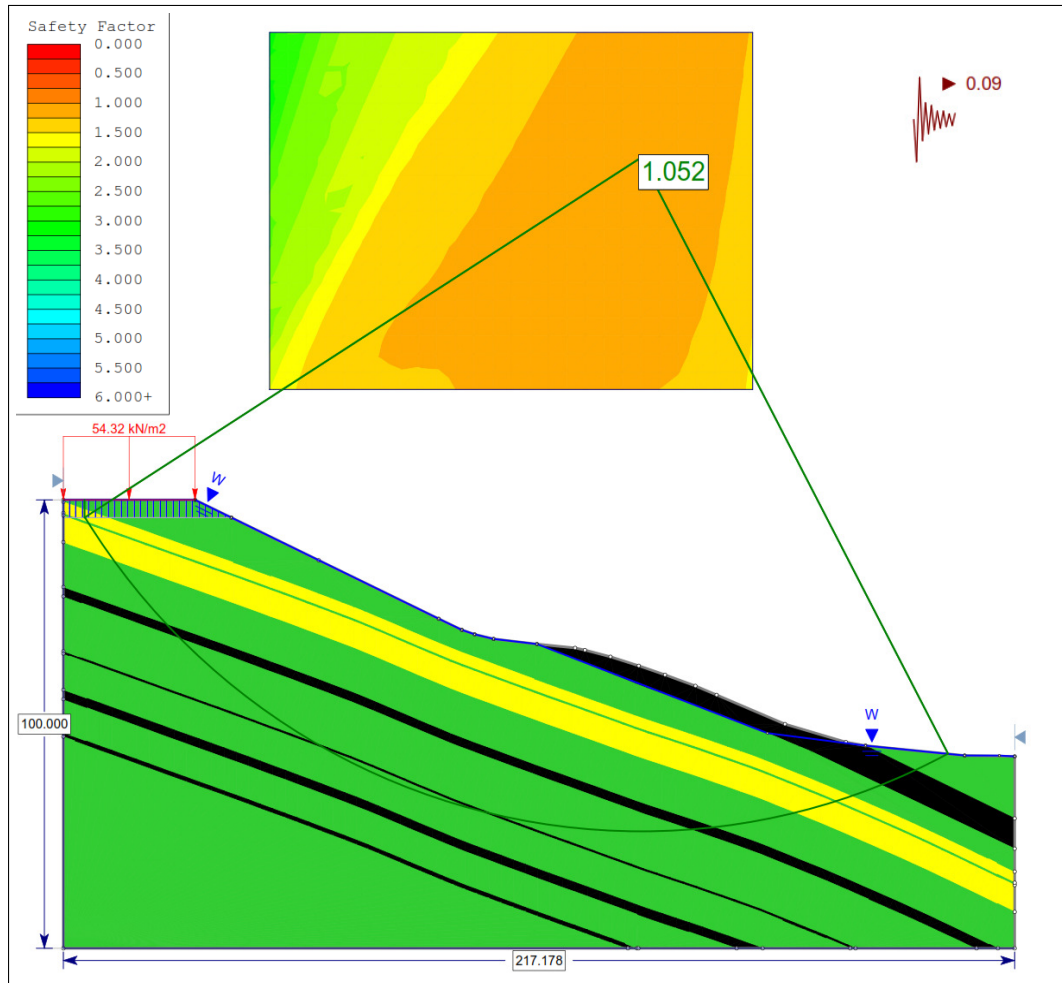


FIGURE 11. Back analysis slope stability model result of LW-4 profile.

in the southern part of the mine pit with a longitudinal orientation trending relatively WSW–ENE. There are 2 highwall segments analyzed, namely the west and east highwall segments. The western highwall slope was analyzed in 2 profiles (West HW-1 and West HW-2), while the eastern highwall slope was analyzed in 4 profiles (East HW-1 to East HW-4). The locations of the six highwall profiles are shown in [Figure 2](#). A typical model from the analysis of the western highwall slope represented by the West HW-1 profile under dynamic conditions is shown in [Figure 12](#), while the eastern highwall slope represented by the East HW-4 profile is shown in [Figure 13](#). The summary of the highwall slope stability analysis is shown in [Table 3](#). In general, the western highwall slope shows a more stable slope than the eastern highwall slope under static and dynamic loading conditions. Two factors influence this: differences in slope geometry and static load conditions. The western highwall has a lower overall slope (about 20–30 meters) with a relatively gentle slope angle (20–23°). There is no static loading because there is no access road for heavy equipment around the slope. On the other hand, the eastern highwall has a relatively high overall slope (about 40–60 meters) with a steeper slope angle (21–38°), and there is static loading because there is mining road access for heavy equipment at the toe, bench, and crest.

The lowwall slope is located in the northern part of the mine pit with a longitudinal orientation trending relatively WSW–ENE, parallel to the highwall slope. Due to the similarity of slope geometry conditions, the slope stability analysis modeling was carried out only on 4 lowwall profiles, namely the LW-1 profile in the west to LW-4 in the east. The location of the lowwall profile is shown in [Figure 2](#). In lowwall, the overall slope geometry has a height ranging from 33–55 meters with a slope angle of 12–22°. A typical model for slope stability analysis LW-4 is shown in [Figure 14](#). The summary of the lowwall slope stability analysis is shown in [Table 4](#). In general, lowwall slopes show stable slope conditions. Under static conditions, all segments of the lowwall slope are in a stable condition. The part of the lowwall slope with the highest probability of failure under dynamic conditions is the slope profile LW-

4, with dynamic FS (deterministic) = 1.170, dynamic FS (mean) = 1.369, and dynamic PoF = 3.2%. This instability was evidenced in the field by several landslides around the slope segment LW-4. The factors that caused instability at this location were shallow groundwater conditions and the overall slope geometry, which is higher and steeper than other profiles.

The results of the slope stability analysis were compared with the slope stability criteria specified in the ESDM Ministry (2018). The summary of the stability conditions of the highwall and lowwall slopes of the research area based on these criteria is shown in [Table 5](#). In static conditions, all slope profiles meet the stability criteria except East HW-4, which has a $FS_{\text{static(deterministic)}} = 1.143$ and a $PoF_{\text{static}} = 12.27\%$. In dynamic conditions, all slope profiles meet the stability criteria except East HW-4, which has a $FS_{\text{dynamic(deterministic)}} = 1.001$ and a $PoF_{\text{dynamic}} = 33.40\%$.

5.3 Recommendation for Slope Optimization

Slope design optimization was carried out on the East HW-4 profile in the eastern highwall slope segment that did not meet the slope stability criteria, as described in the previous section. Slope optimization was carried out in 2 ways, namely by lowering the groundwater level or reducing the overall slope angle, while other parameters were constant. Slope optimization was only carried out under dynamic conditions, assuming that if the slope meets the stability criteria under dynamic conditions, the slope would be stable in static conditions. The results of the optimization of the slope of East HW-4 are shown in [Table 6](#) and [Table 7](#).

6 CONCLUSION

In this study, evaluations of geological engineering conditions and slope stability analysis were carried out in the west pit of the coal mine of PT. TMR. The geological engineering conditions analyzed were geomorphological conditions, rock conditions, geological structures, and groundwater level. Back analysis performed on the northern lowwall slope segment showed that the slope was critical by reducing the claystone peak shear strength parameter by 20%. The parameters of the back analysis were

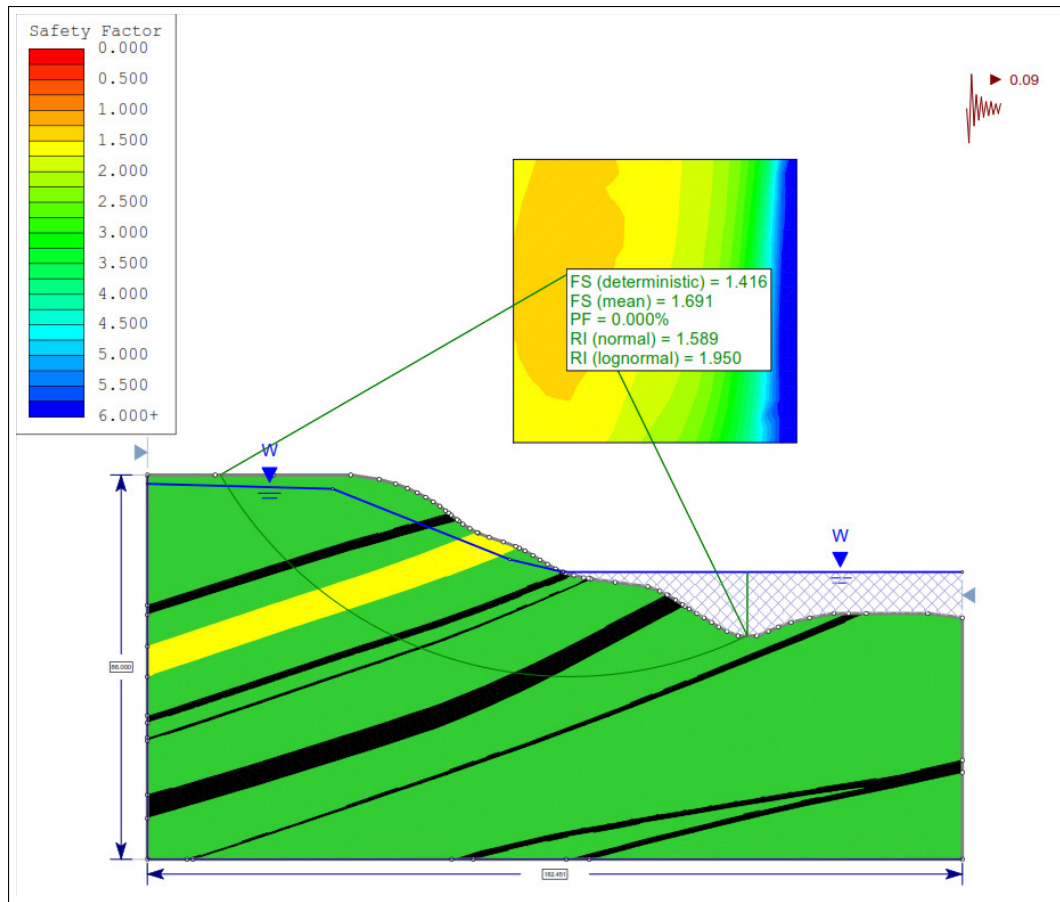


FIGURE 12. Slope stability model of West HW-1 profile under dynamic loading.

TABLE 3. Summary of highwall slope stability analysis results.

| Profile | Slope geometry | | Static FS (Deterministic) | Static FS (Mean) | Static PoF (%) | Dynamic FS (Deterministic) | Dynamic FS (Mean) | Dynamic PoF (%) |
|-----------|----------------|-----------------|---------------------------|------------------|----------------|----------------------------|-------------------|-----------------|
| | Height (m) | Slope angle (°) | | | | | | |
| West HW-1 | 31 | 23 | 1.867 | 2.224 | 0.00 | 1.416 | 1.691 | 0.00 |
| West HW-2 | 20 | 20 | 1.714 | 2.007 | 0.00 | 1.323 | 1.544 | 0.00 |
| East HW-1 | 60 | 21 | 1.604 | 1.874 | 0.00 | 1.197 | 1.403 | 1.70 |
| East HW-2 | 51 | 25 | 1.355 | 1.593 | 0.00 | 1.086 | 1.282 | 13.20 |
| East HW-3 | 49 | 24 | 1.478 | 1.660 | 0.00 | 1.251 | 1.416 | 0.50 |
| East HW-4 | 41 | 38 | 1.143 | 1.344 | 12.27 | 1.001 | 1.179 | 33.40 |

TABLE 4. Summary of lowwall slope stability analysis results.

| Profile | Slope geometry | | Static FS (Deterministic) | Static FS (Mean) | Static PoF (%) | Dynamic FS (Deterministic) | Dynamic FS (Mean) | Dynamic PoF (%) |
|---------|----------------|-----------------|---------------------------|------------------|----------------|----------------------------|-------------------|-----------------|
| | Height (m) | Slope angle (°) | | | | | | |
| LW-1 | 36 | 22 | 1.654 | 2.021 | 0.00 | 1.292 | 1.583 | 0.90 |
| LW-2 | 33 | 13 | 2.217 | 2.631 | 0.00 | 1.553 | 1.851 | 0.00 |
| LW-3 | 36 | 12 | 2.284 | 2.727 | 0.00 | 1.581 | 1.867 | 0.00 |
| LW-4 | 55 | 20 | 1.503 | 1.773 | 0.00 | 1.17 | 1.369 | 3.20 |

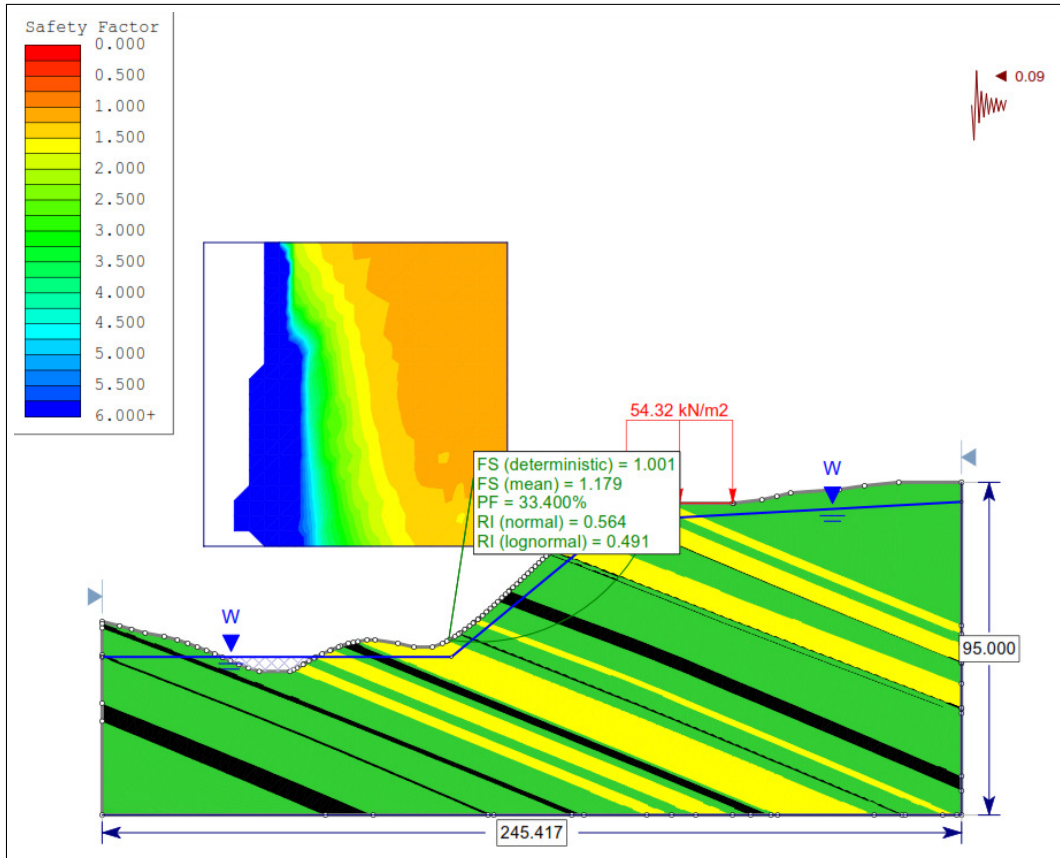


FIGURE 13. Slope stability model of East HW-4 profile under dynamic loading.

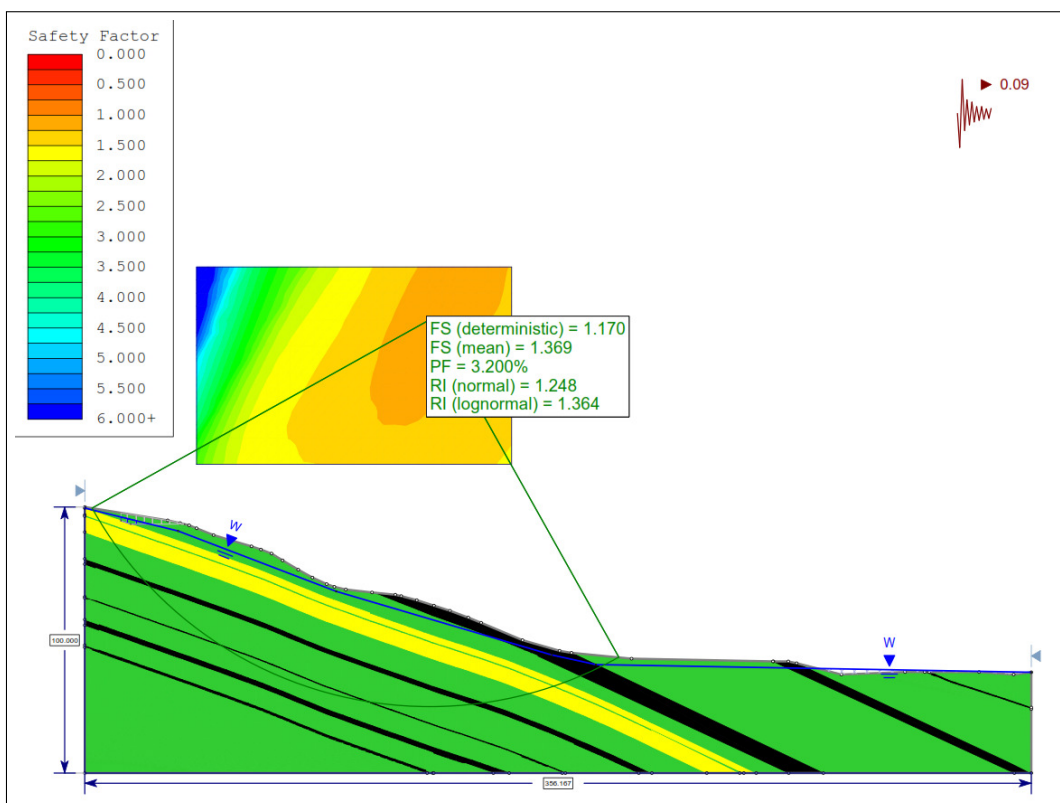


FIGURE 14. Slope stability model of LW-4 profile under dynamic loading.

TABLE 5. The summary of the stability conditions of the highwall and lowwall slopes of the research area based on ESDM Ministerial Decree No. 1827 K/30/MEM/2018 (ESDM Ministry, 2018).

| Profile | Static FS (Deterministic) | Static FS (Mean) | Static PoF (%) | Meets slope stability criteria* | Dynamic FS (Deterministic) | Dynamic FS (Mean) | Dynamic PoF (%) | Meets slope stability criteria* |
|-----------|---------------------------|------------------|----------------|---------------------------------|----------------------------|-------------------|-----------------|---------------------------------|
| LW-1 | 1.654 | 2.021 | 0.00 | Yes | 1.292 | 1.583 | 0.90 | Yes |
| LW-2 | 2.217 | 2.631 | 0.00 | Yes | 1.553 | 1.851 | 0.00 | Yes |
| LW-3 | 2.284 | 2.727 | 0.00 | Yes | 1.581 | 1.867 | 0.00 | Yes |
| LW-4 | 1.503 | 1.773 | 0.00 | Yes | 1.17 | 1.369 | 3.20 | Yes |
| West HW-1 | 1.867 | 2.224 | 0.00 | Yes | 1.416 | 1.691 | 0.00 | Yes |
| West HW-2 | 1.714 | 2.007 | 0.00 | Yes | 1.323 | 1.544 | 0.00 | Yes |
| East HW-1 | 1.604 | 1.874 | 0.00 | Yes | 1.197 | 1.403 | 1.70 | Yes |
| East HW-2 | 1.355 | 1.593 | 0.00 | Yes | 1.086 | 1.282 | 13.20 | Yes |
| East HW-3 | 1.478 | 1.66 | 0.00 | Yes | 1.251 | 1.416 | 0.50 | Yes |
| East HW-4 | 1.143 | 1.344 | 12.27 | No | 1.001 | 1.179 | 33.40 | No |

*slope stability criteria referring to the Minister of Energy and Mineral Resources Decree No. 1827 K/30/MEM/2018

TABLE 6. Optimization of East HW-4 slope by lowering the groundwater level.

| Slope condition | Overall slope height (m) | Overall slope angle (°) | Dynamic FS (deterministic) | Dynamic FS (mean) | Dynamic PoF (%) | Meet slope stability criteria |
|--------------------|--------------------------|-------------------------|----------------------------|-------------------|-----------------|-------------------------------|
| Actual GWL | 41 | 38 | 1.001 | 1.179 | 33.4 | No |
| GWL lowered by 2 m | 41 | 38 | 1.052 | 1.228 | 19.9 | No |
| GWL lowered by 3 m | 41 | 38 | 1.078 | 1.256 | 16.0 | No |
| GWL lowered by 4 m | 41 | 38 | 1.102 | 1.283 | 13.3 | Yes |

TABLE 7. Optimization of East HW-4 slope by reducing the angle of the overall slope.

| Slope condition | Overall slope height (m) | Overall slope angle (°) | Dynamic FS (deterministic) | Dynamic FS (mean) | Dynamic PoF (%) | Meet slope stability criteria |
|---------------------------|--------------------------|-------------------------|----------------------------|-------------------|-----------------|-------------------------------|
| Actual geometry | 41 | 38 | 1.001 | 1.179 | 33.4 | No |
| Crest pushed back by 5 m | 41 | 36 | 1.026 | 1.213 | 26.4 | No |
| Crest pushed back by 10 m | 41 | 33 | 1.102 | 1.302 | 16.3 | No |
| Crest pushed back by 13 m | 41 | 32 | 1.090 | 1.290 | 15.1 | No |
| Crest pushed back by 15 m | 41 | 31 | 1.111 | 1.309 | 11.9 | Yes |

used in the stability analysis of 10 lowwall and highwall slope profiles which showed that all slope profiles met the stability criteria except the East HW-4 profile, which was on the eastern highwall. In static conditions, all slope profiles met the stability criteria except East HW-4, which has a static FS (deterministic) = 1.143 and a static PoF = 12.27%. In dynamic conditions, all slope profiles met the stability criteria except East HW-4, which has a dynamic FS (deterministic) = 1.001 and a dynamic PoF = 33.40%. In this profile, it is recommended to optimize the slope with 2 alternatives: lowering the GWL elevation by 4 meters from the actual condition or reducing the overall slope angle to 31°.

ACKNOWLEDGEMENTS

The authors would like to thank PT. TMR for granting research permission, providing secondary data, and supporting the primary data collection process. The first author would also like to thank Mr. Hendra Santoso, who has assisted in the field data acquisition process.

REFERENCES

- Abdulai, M., Sharifzadeh, M. (2019) Uncertainty and Reliability Analysis of Open Pit Rock Slopes: A Critical Review of Methods of Analysis, *Geotech Geol Eng* (2019), 37: 1223-1247.
- Abramson, W.L., Lee, T.S., Sharma, S., Boyce, G.M. (2002) *Slope Stability and Stabilization Methods* 2nd ed., New York: John Wiley & Sons, Inc., 712.
- Bachtiar, A. (2004) Kerangka Stratigrafi Sekuen dan Karakter Batuan Induk Miosen Awal di Cekungan Kutai Hilir, Kalimantan Timur, Doctoral Dissertation, Institut Teknologi Bandung.
- Bachtiar, A., Nugroho, D.H.H., Azzaino, Z., Utomo, W., Krisyuniyanto, A., Sani, M. (2013a) Surface Data Re-evaluation, Eocene Source Rock Potential and Hydrocarbon Seepage, And Eocene Sand Reservoir Prospectivity in West Sangatta Northern Kutai Basin, Proceedings Indonesian Petroleum Association, 37th Annual Convention & Exhibition, 6.
- Bachtiar, A., Purnama, Y.S., Suandhi, P.A., Krisyuniyanto, A., Rozalli, M., Nugroho, D.H.H., Suleiman, A. (2013b) The Tertiary Paleogeography of the Kutai basin And Its Unexplored Hydrocarbon Plays, in Proceedings Indonesian Petroleum Association, 37th Annual Convention & Exhibition. Bell, F.G. (2007) *Engineering Geology*, 2nd ed., Elsevier, 581.
- Bergbauer, S., Pollard, D. D. (2004) A new conceptual fold-fracture model including pre-folding joints, based on the Emigrant Gap anticline, Wyoming: *Geological Society of America Bulletin*, v. 116, no. 3/4, 294-307.
- Cloke, I.R., Moss, S.J., Craig, J. (1999) Structural Controls on the evolution of the Kutai Basin, East Kalimantan, *Journal of Asian Earth Sciences*, 137-156.
- Davis, G. H., Reynolds, S. J., Cluth, C. (2012) *Structural geology of rocks and regions*, Wiley, Hoboken, 839.
- ESDM Ministry (2018) Keputusan Menteri Energi Dan Sumber Daya dan Mineral Nomor 1827 K/30/MEM/2018 Tentang Pedoman Pelaksanaan Kaidah Teknik Pertambangan Yang Baik, 370.
- Gonzalez de Vallejo, L.G., Ferrer, M. (2011) *Geological Engineering*, Boca Raton: CRC Press, 669.
- Howard, A.D. (1967) Drainage Analysis in Geologic Interpretation: A Summation, in *American Association of Petroleum Geologist Bulletin*, 51, 2246-2259.
- Ikatan Ahli Geologi Indonesia (IAGI) (1996) *Sandi Stratigrafi Indonesia*, IAGI, 34.
- Lorig, L., Stacey, P., Read, J. (2010) Slope Design Method, in Read, J. Stacey, P. (eds), *Guidelines for Open Pit Slope Design*, CSIRO Publishing, 237-264.
- Morgenstern, N.R., Price, V.E. (1965) The Analysis of the Stability of General Slip Surfaces. *Géotechnique*, 15, 79-93.
- Moss, S.J., Chambers, J.L.C. (1999) Tertiary facies architecture in the Kutai Basin, Kalimantan, Indonesia, in *Journal of Asian Earth Sciences* 17 (1999). 157-181.
- Nuay, E.S., Astarita, A., Edwards., K. (1985) Early Middle Miocene Deltaic Progradation in the Southern Kutai Basin, in 14th Annual IPA Convention Proceedings (Volume I), 63-81.
- Saksono, R.T. (2022) Evaluasi Kestabilan Lereng Tambang Batubara di Pit Barat PT. Tawabu Mineral Resource, Kalimantan Timur, Magister Teknik Geologi UGM (Thesis). 474.
- Sandria, G.J. (2014) Geologi Dan Perhitungan Sumberdaya Batubara Dengan Metode Cross Section Daerah Sepaso Selatan, Kecamatan Bengalon Kabupaten Kutai Timur, Provinsi Kalimantan Timur (Thesis summary), UPN "Veteran" Yogyakarta. 8.
- Santoso, H. (2002) Evaluasi Stabilitas Lereng dan Prediksi Volume Material Longsor Tambang Batubara PT. Tawabu Mineral Resource Provinsi Kalimantan Timur, Magister Teknik Geologi UGM (Thesis). 637.
- Schneider, H.R. (1997) Definition and characterization of soil properties, in Proceedings XIV International Conference on Soil Mechanics and

- Geotechnical Engineering, Hamburg, Balkema, Rotterdam, 2271-2274.
- Stacey, P. (2010) Fundamentals of Slope Design, in Read, J. Stacey, P. (eds), Guidelines for Open Pit Slope Design, CSIRO Publishing, 1-14.
- Stearns, D. W. (1968) Certain aspects of fractures in naturally deformed rock, dalam Riecker, R. E. (ed.), NSF Advanced Science Seminar in Rock Mechanics, Air Force Cambridge Research Laboratories Special Report, Bedford, MA, 97-118.
- Steffen, O.K.H., Terbrugge, P., Venter, J. (2008) A risk evaluation approach for pit slope design, Johannesburg: ARMA American Rock Mechanics Association.
- Sukardi, Sikumbang, N., Umar, I., Sunaryo, R. (1995) Peta Geologi Lembar Sangatta, Kalimantan Skala 1:250.000, Bandung: Pusat Penelitian dan Pengembangan Geologi.
- Tapia, A., Contreras, L.F., Jefferies, M., dan Steffen, O. (2007) Risk Evaluation of Slope Failure at the Chuquicamata Mine, in Proceedings of the 2007 International Symposium on Rock Slope Stability in Open Pit Mining and Civil Engineering, Perth, Australia, 1-12.
- Ulusay, R. (2013) Harmonizing Engineering Geology With Rock Engineering For Assessing Rock Slope Stability, ISRM SINOROCK 2013, Shanghai.
- _____ (2019) Harmonizing Engineering Geology With Rock Engineering For Assessing Rock Slope Stability: A Review Of Current Practice, Geoteknika, Tuzla: Društvo za geotekniku u Bosni i Hercegovini, 1-16..